Somma Vesuvius: the Volcano and the Observatory

Field trip guidebook – REAKT

Mauro Antonio Di Vito, Monica Piochi, Angela Mormone, Anna Tramelli

Istituto Nazionale di Geofisica e Vulcanologia, sezione Osservatorio Vesuviano

Field Leaders

Mauro Antonio Di Vito, Monica Piochi

Naples, September 22th, 2011

Pubblicazione di AMRA S.c. a r.l.
Via Nuova Agnano 11, Napoli
www.amracenter.com

Realizzazione
doppiavoce
www.doppiavoce.it

Finito di stampare a Napoli nel mese di settembre 2011 presso Officine Grafiche Francesco Giannini & Figli S.p.A.

PREFACE

The present guidebook was prepared for the fieldtrip during the Kick off meeting of the project titled *"Strategies and tools for Real Time Earthquake RisK ReducTion" (REAKT)*. It reports information on the geology of the Somma-Vesuvius volcanic area and illustrates the sites visited during the field excursion. The guide mostly benefited of contributions coming from some previous guidebooks (Cioni et al., 1995; Orsi et al., 1998); it also includes some interesting results available in the main and most recent literature. The fieldtrip will be devoted to illustrating i) the major morphological and structural features of the Somma-Vesuvius volcano, and ii) the deposits of the eruptions and their impact on the territory. The trip will end with the tour of the Osservatorio Vesuviano edifice that preserves the memory of the oldest volcanological observatory in the world and hosts a museum and two scientific exibitions.

INTRODUCTION

Somma-Vesuvius (Fig. 1) is an active volcano, one of the most dangerous on the Earth. More than half a million people live in a nearly continuous belt of towns and villages built around the volcano, in the area immediately threatened by possible future eruptions. The knowledge of the present state of the volcano, which is fundamental for recognizing unrest phenomena and for evaluating possible future pre-eruptive scenarios, mostly derives from petrological and geophysical studies. The most recent ones (e.g., Auger et al., 2001; De Natale et al., 2001; Lima et al., 2003; Marianelli et al., 1999) indicate the existence of magma storage located at ~10 km depth bsl. The occurrence of magma storage at shallower crustal levels, although not pointed out by geophysical investigations, has been suggested on the basis of both sedimentological (e.g., Barberi and Leoni, 1980) and fluid inclusion data (Belkin and De Vivo, 1993; Cioni, 2000).
At present, Mount Vesuvius is quiescent after 300 years of almost continuous volcanism, which ended with the 1944 eruption. Its present activity consists of earthquakes, with hypocenters located beneath the central crater down to 6 km depth bsl (Vilardo et al., 1999), and of fumarolic emissions maily concentrated in the crater area (Chiodini et al., 2001). Thermal modelling (Quareni et a., 2007) suggested that volatile degassing (mainly CO_2) is the first rank process responsible for the cooling of magma within the conduit, left essentially full after the end of deep-derived magma supply, which could have generated the transition from the pre-1944 open conduit to the present closed conduit regime.

Figure 1. Aerial view of Somma-Vesuvius volcano. Red dots are the location of stops.

Regional geologic setting

The Mount Somma-Vesuvius is a strato-volcano located in the Campanian Plain, together with the volcanic fields of Campi Flegrei, Ischia and Procida. These volcanoes are part of the Campanian Comagmatic Province that belongs to the potassium-rich Italian belt. In particular, the Campanian Plain is a structural depression delimited by the Southern Apennines to the east, south and north, and by the Tyrrhenian Sea, to the west (Figs. 2 and 3). The Apennines chain results from compressive deformation of the African continental margin. It is composed of a pile of tectonic thrusts made up of Triassic to Pliocene sedimentary rocks (Fig. 3) belonging to a variety of Mesozoic and Palaeogenic palaeogeographic domains (D'Argenio et al., 1973) and overlying a crystalline-metamorphic basement. After a compressive tectonic phase from Cretaceous to Pliocene, the western side of the Chain was affec-

Figure 2. Satellite imagery of the Campanian Plain and the Neapolitan Volcanoes.

ted by extensional tectonics (e.g., Doglioni, 1991) that displaced, at variable depths below the Campanian Plain, all the upper sedimentary succession. Actually, 2-3,000 m thick sequences of Plio-Quaternary continental, deltaic, and marine sediments, intercalated with volcanic deposits has been found by drilling at ~1.4 km (Trecase well 1 site) beneath the Mount Somma-Vesuvius edifice and identified by seismic profiles at depths >3-4 km bsl in the Gulf of Naples (Piochi et al., 2004 and references therein).

The regional stress regime, which has determined the formation of the Campanian Plain, generated NW-SE and NE-SW trending normal faults and also favoured rise of the magmas. With the exception of oldest volcanic rocks with calc-alkaline composition, erupted magmas are younger than 400 ka and alkaline (Fig. 4); high potassium compositions were erupted only at the Vesuvius (Piochi et al., 2004 and references therein). The Procida Island ended its volcanism at 18 ka (De Astis et al., 2004). Historical eruptions (Fig. 4) have occurred at Ischia (from VII century BC to 1302 AD) (de Vita et al., 2010), Campi Flegrei (1538 AD) (Di Vito et al., 1999), and Vesuvius (from 79 AD to 1944) (Santacroce et al., 2008).

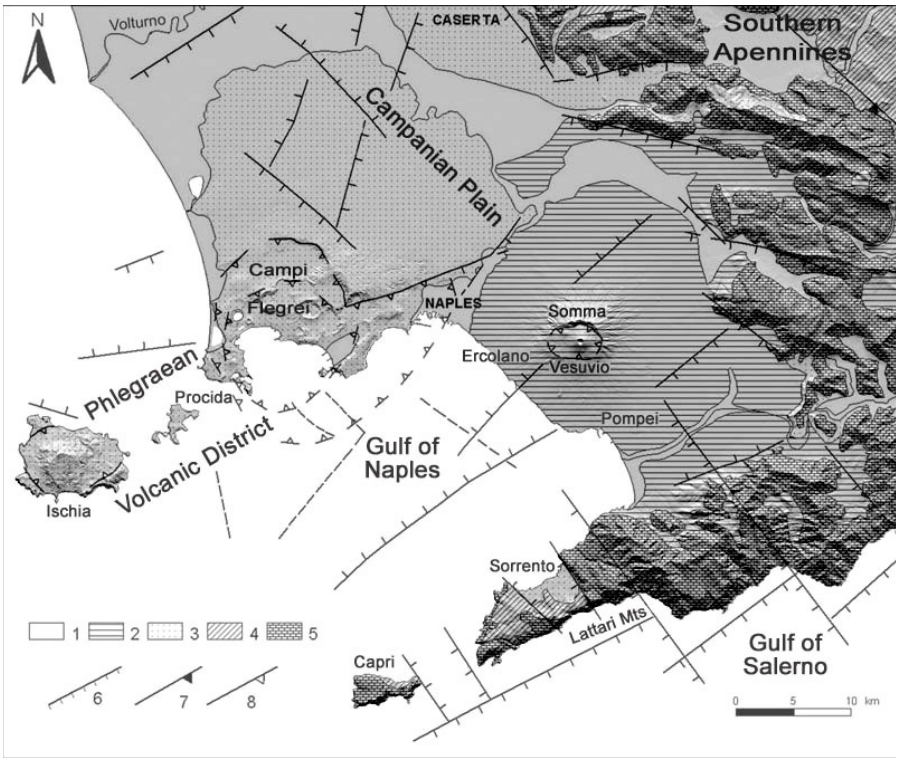

Figure 3. Geological sketch map of the Neapolitan area of the Campanian Plain. 1) Quaternary and active terrigenous sediments; 2) Somma-Vesuvius volcanics; 3) Phlegraean District volcanics; 4) Pliocene and Miocene terrigenous sediments; 5) Mesozoic carbonate units; 6) faults; 7) overthrusts; 8) caldera margins.

SOMMA-VESUVIUS

Volcanology

The Somma-Vesuvius is a moderate size (1281 m asl) composite central volcano (Fig. 1). It consists of an older volcano, Monte Somma, dissected by a summit caldera, and Mount Vesuvius, a recent cone developed within the oldest Somma caldera (Fig. 5), and possibly grown after the AD 79 "Pompeii" eruption. Actually, the Roman name Vesuvius (or Vesubius) was referring to the volcano, and only since the Vth century, chroniclers make mention of Mt Somma, as the highest ("summa") peak of the mountain.

The caldera has a complex shape resulting from several collapses, each related to a high-explosive plinian eruption (Cioni et al., 1999). It has a quasi-

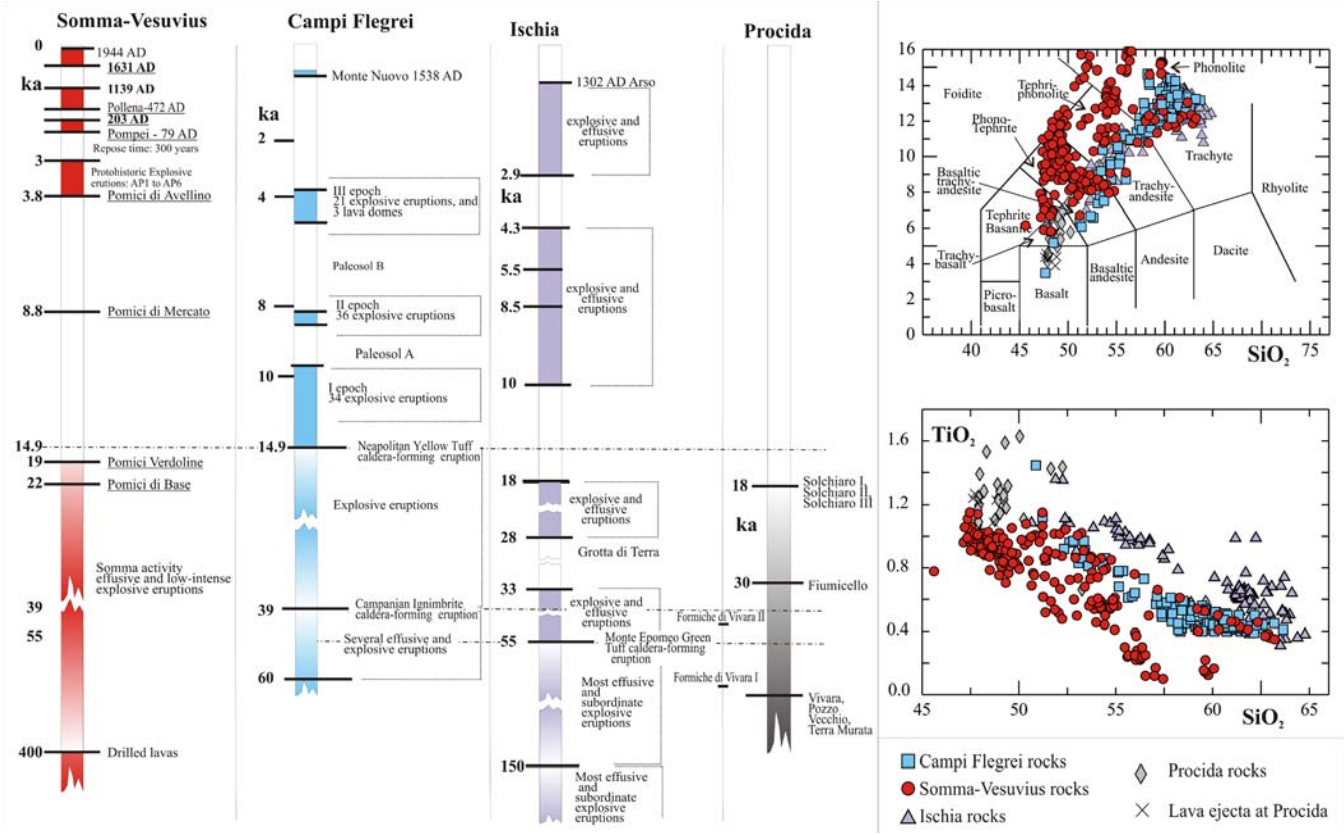

Figure 4. Timing and compositions of volcanism at the Somma-Vesuvius, Ischia, Procida and Campi Flegrei, within the Campanian area.

elliptical shape with a 5-km-long, east-west major axis (Fig. 5). Its northern rim is a well-defined 300 m high steep wall with an average elevation of approximately 1000 m asl. Its southern part runs from the eastern Cognoli di Levante to the southeastern tip of Piano delle Ginestre (Fig. 1) and is evidenced by a sharp increase in the inclination slope below ~600 m asl (Fig. 5). Here the structure is covered by a pile of recent lava flows and pyroclastic deposits that, after filling the caldera, overtopped its lowest rim.

Along the caldera wall a pile of lava flows, spatter and scoria deposits are exposed (Figs 4, 6) (Santacroce and Sbrana, 2003) and reflect a dominant effusive activity (Johnston Lavis, 1884; Santacroce, 1987) that prevailed on the explosive, generally low energy events (Cioni et al.,1999). The products of this older (>22 ka) explosive activity are exposed in medial and distal outcrops on the Apennine Chain, always intercalated between the Campanian Ignimbrite (from the nearby Campi Flegrei; Fig. 4) and the Pomici di Base (from Somma-Vesuvius) deposits. One of these medial-distal fallout deposits has been related to a compositionally similar thick pyroclastic unit, penetrated by a borehole nearby Camaldoli della Torre eccentric apparatus (Di Renzo et al., 2007; Di Vito et al. 2008). The specific sedimentological characteristics suggest the occurrence of high-intesity explosive volcanism in the Vesuvius area just after the emplacement of the Campanian Ignimbrite (Di Renzo et al., 2007).

The history of the volcano after 22 ka has been characterized either by long quiescence periods, interrupted by Plinian or sub-Plinian eruptions, or by periods of persistent volcanic activity (Figs 4, 7), with lava effusions and Strombolian to phreato-magmatic eruptions, related to the alternation of closed and open conduit conditions, respectively. In particular, the growth of the Vesuvius cone has taken place, although with some minor summit collapses, during periods of persistent low-energy open-conduit activity, the last of which occurred between 1631 and 1944 (Arrighi et al., 2001). The total volume of erupted magmas has been estimated to be ~300 km^3 (Civetta and Santacroce, 1992).

The earliest well-known Plinian eruption (Pomici di Base; 22 ka; Cioni et al., 1999 and references therein) determined the beginning of both collapse of the Mt. Somma volcano and formation of the caldera. This eruption was followed by lavas effusions that flowed along the eastern slopes of the volcano, and a quiescent period interrupted at 19 ka bp by the Pomici Verdoline sub-Plinian eruption. The subsequent long period of quiescence, during which only two low-energy eruptions took place, lasted until 8.8 ka bp, when it was broken by the Plinian Pomici di Mercato eruption (Cioni et al., 1999; Mele et al., 2011). A thick paleosol overlying the deposit of this eruption testifies for a further period of quiescence, interrupted only by two low-energy eruptions. This paleosol contains many traces of human presence until the Early Bronze

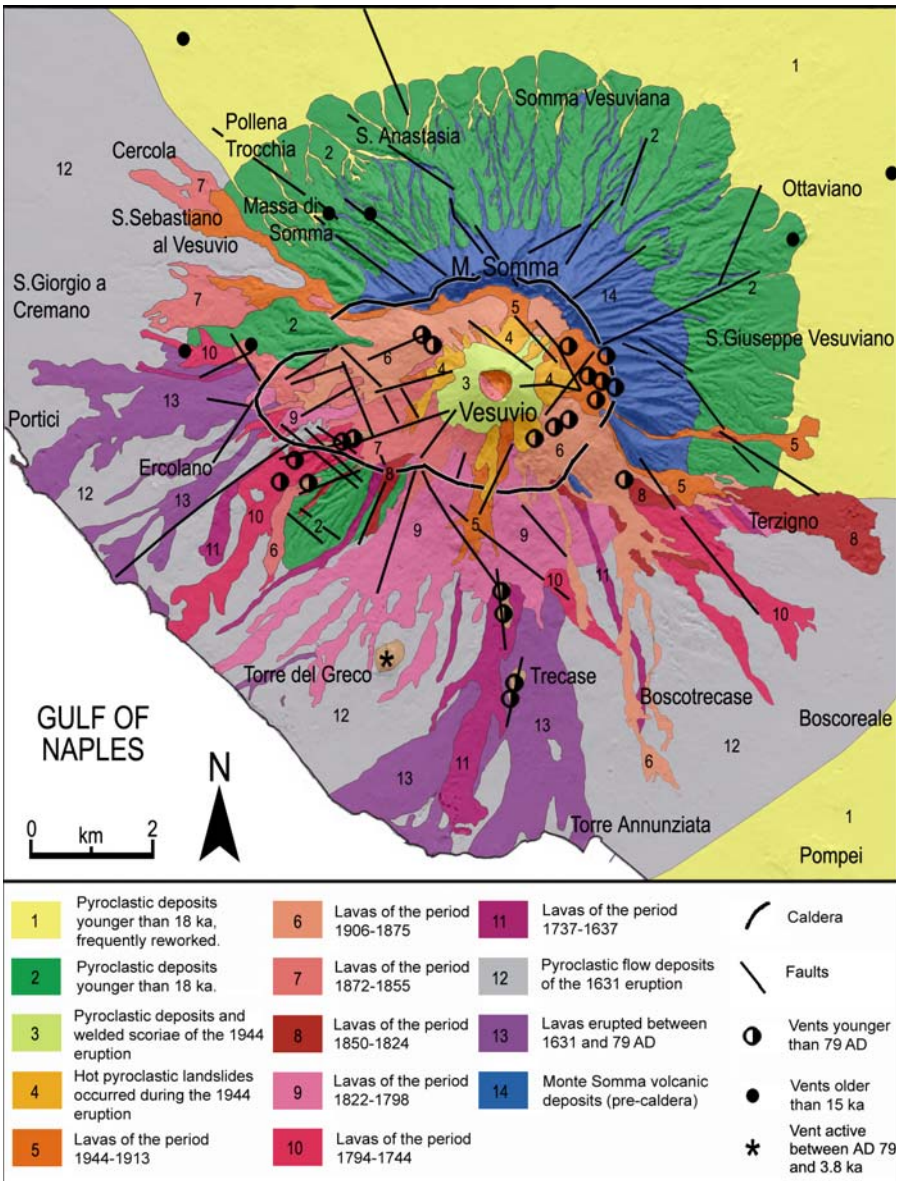

Figure 5. Somma-Vesuvius geological sketch map (after Orsi et al, 2003a. Structural lineaments after Ventura and Vilardo al., 1999).

Figure 6. Monte Somma caldera scarp. View from the South.

age, and is covered by the deposits of the Plinian Pomici di Avellino eruption (3.8 ka) (Cioni et al., 1999; Di Vito et al., 2009).
The Pomici di Avellino eruption was characterized for three principal phases (opening, Plinian and phreatomagmatic) and five eruptive units (EU1-5, Fig. 7) (Sulpizio et al., 2010). The opening phase of the eruption, which saw the formation of a short-lived, low and pulsating eruptive column, produced EU1 unit that distributed to the NE, at a distance of several tens of km from the volcano. The overlying EU2, 3 and 4 were deposited in the principal phase of the eruption by a sustained Plinian eruptive column, which reached a maximum height of about 30 km. These products consist of white, and then grey, pumice fallout deposits (EU2-3) distributed again towards the NE, covering an area of more than 15,000 km^2 (Fig. 8). Due to their distribution, they cover the famous Nola village, but none of them were found in the vicinity of the Afragola, which suffered only from the effects of the final succession deposition (Di Vito et al., 2009). This last unit, EU5, generated by repeated phreatomagmatic explosions, derived by dilute, turbulent pyroclastic current, distributed mainly to the WNW, at a distance >25 km from the volcano. Fine ash elutriated by these currents was dispersed over distances of several hundred km to the NW (Sulpizio, et al., 2008). The emplacement temperatures of these currents were estimated between 250 and 300 °C. After the eruption, diverse floods emplaced variable sized finely-laminated sand deposits in the Campanian Plain.
The he study of the cited Ancient Bronze age villages allowed evaluating the effects of emplacement of the Pomici di Avellino deposits, with particular reference to the pyroclastic currents (Di Vito et al., 2009). The lower of these is a massive fine-ash deposit with accretionary lapilli and abundant imprints of vegetation; it exhibits notable variations in thickness in correspondence

to obstacles and irregularities of the underlying surface. Buildings were penetrated by the currents and the spaces between the reeds in the huts' thatch were completely filled. Furthermore, some buildings suffered damage, in particular to their more elevated parts. As palaeotemperature measurements have confirmed, a lull of several hours followed the massive fine-ash deposition and permitted its cooling down sufficiently to allow the passage of men and animals that left large. Stamping leaved deep imprints on the ash deposits (Fig. 9), which was filled in and preserved by larger-sized material of the following units. They consists of a succession of coarse-, medium- and fine-ash layers, and tends to mantle buildings and increase in thickness close up to them. The larger buildings collapsed during this phase, probably due to the destabilizing effects of heavy ash loads on the weakened structures. The following units have similar characteristics, but they are less coarse and exhibits a rapid lateral transition to fine-ash deposits. Notably, all the surfaces of the described sequence was abundantly deformed by animal hoof-prints and human footprints formed at a time when the deposit was still highly plastic, with a mud-like consistency. It is interesting to note that the pyroclastic currents did not cause the immediate collapse of many small buildings and some larger ones and did not blow over fences or trees. Buildings generally fell down due to the weight of volcanic ash accumulated on roofs and in some cases it is likely that they were subsequently kept in an upright position by the consolidating volcanic ash which surrounded the lower parts of supporting posts; this latter effect seems to have applied to all the fences.

The Pomici di Avellino eruption was followed by at least 8 Strombolian to sub-Plinian eruptions, over a relatively short time, and by about three centuries of quiescence, broken by the Plinian AD 79 eruption (Andronico and Cioni, 2001 and references therein), the description of which is in the later

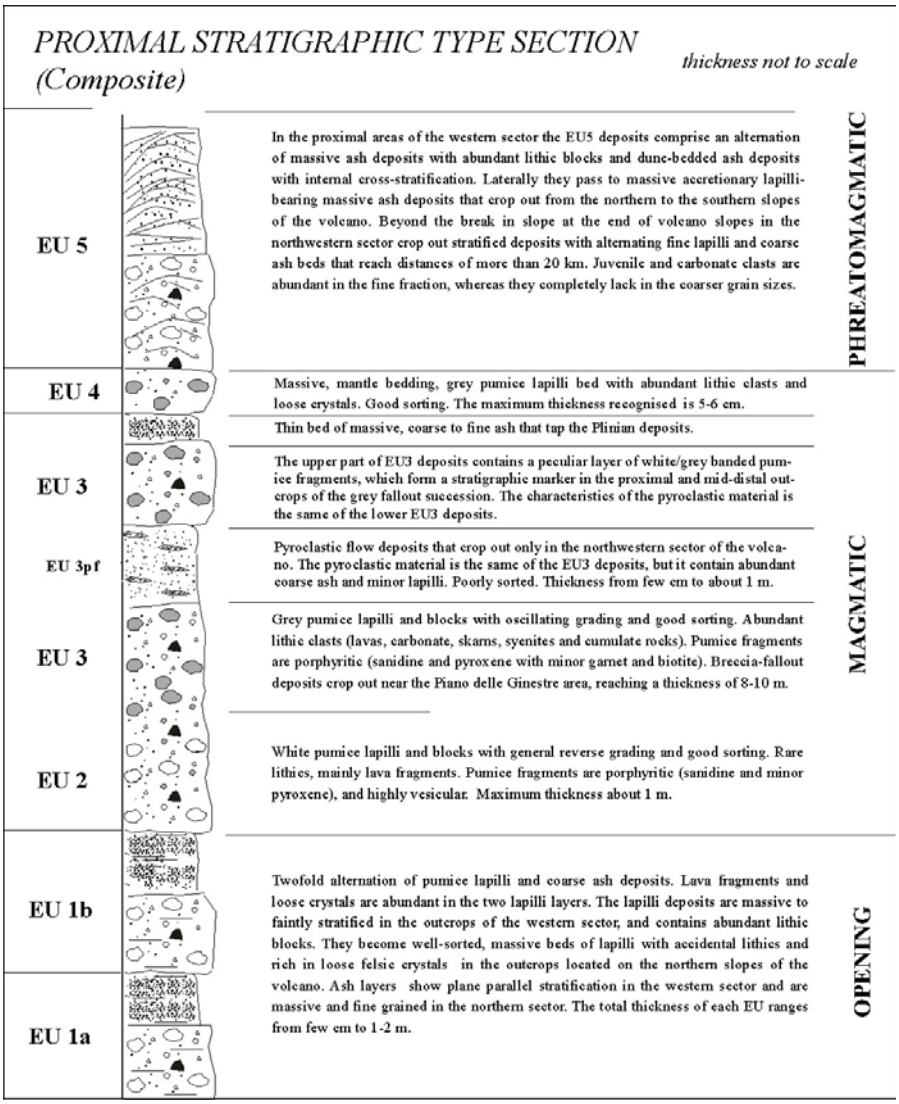

Figure 7. Type section of the Pomici di Avellino deposits (EU – eruptive unit, see text).

stop 1 section. After this eruption, the volcano has generated only two more sub-Plinian events in AD 472 (Rosi and Santacroce, 1983) and 1631 (Rolandi et al., 1993; Rosi et al., 1993), and low-energy open-conduit activity between the 1st and 3rd, 5th and 8th, 10th and 11th centuries, and 1631 and 1944 (Arrighi et al., 2001). Since last eruption of 1944, Vesuvius is quies-

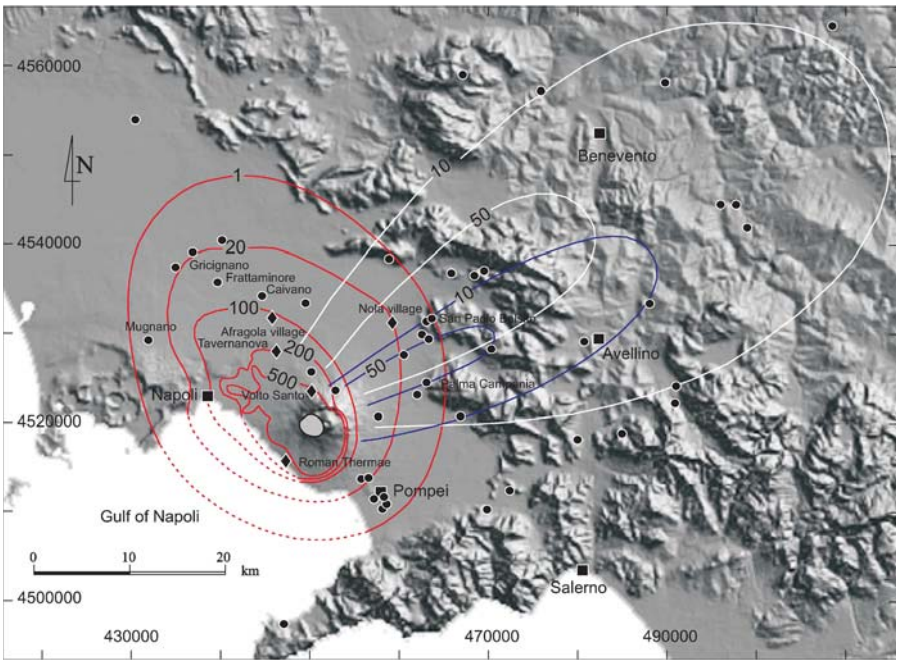

Figure 8. Distribution of the Pomici di Avellino deposits. Isopachs in cm: blue=EU2, White=EU3, red=EU5. Light gray area= inferred vent. Dot and rhomb (except Roman Thermae) = Bronze age sites and villages (modified after Di Vito et al., 2009). Roman Thermae was a sampling site for paleotemperature measurements.

cent, as it has not shown signs of unrest and only moderate seismicity and fumaroles testify its activity.

All Plinian eruptions of Somma-Vesuvius were characterized by vent opening, sustained column and pyroclastic flow and/or surge phases, and were accompanied by volcano-tectonic collapses. Sustained columns, which reach maximum heights of about 30 km, generated widespread fallout deposits (1.5-4.4 km^3, DRE) (Fig. 10). Pyroclastic currents (0.25 and 1 km^3, DRE) are distributed along the volcano slopes and within the surrounding plains, reaching maximum distances of over 20 km from the vent (Fig. 10) (Cioni et al., 2003; Gurioli et al., 2010). In proximal areas, thick breccia deposits were produced during the caldera collapse. Among the sub-Plinian eruptions of Vesuvius, only the AD 472 and the 1631 events are studied in details (Rosi and Santacroce, 1983; Rolandi et al., 1993; Rosi et al., 1993). They are characterized by alternation of sustained columns and pyroclastic flow and/or surge generation. Sustained columns are less than 20 km high and

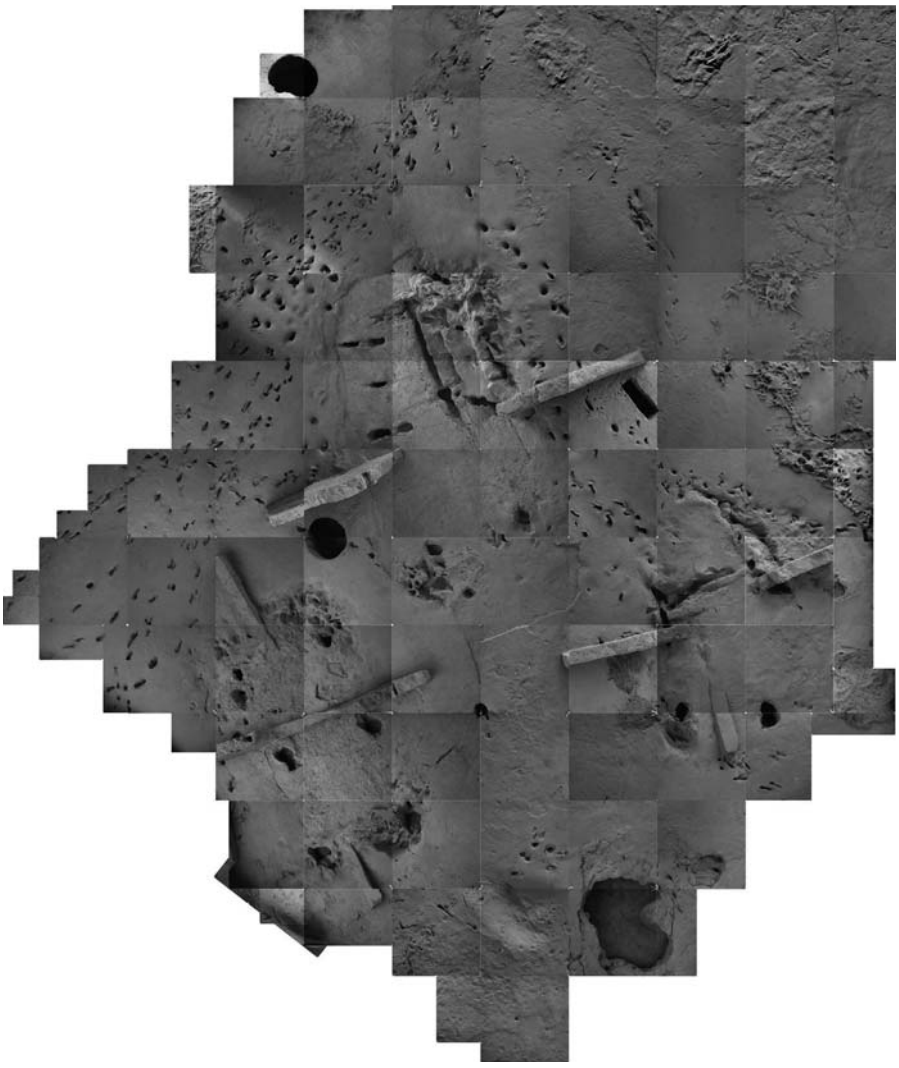

Figure 9. Human foot-prints on the EU5 lower unit (see text) (after Di Vito et al., 2009).

pyroclastic currents travel distances not in excess of 10 km. Fallout deposits of both Plinian and sub-Plinian eruptions are generally dispersed to the east of the volcano, depending on the main wind directions (Cioni et al., 2003) (Fig. 10). The occurrence of a caldera collapse may be related to the partial or complete emptying of the magma chamber. Each eruption shows trace of the intervention, during the caldera collapse phases, of fluids from the hydro-

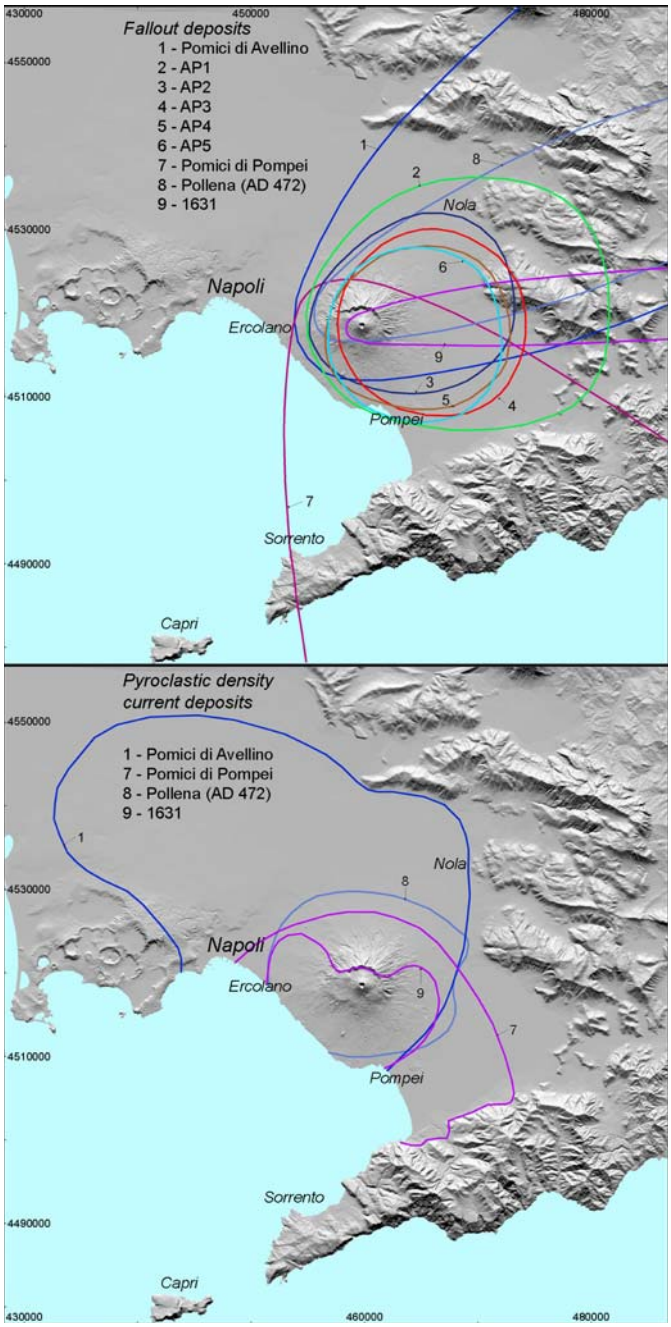

Figure 10. Distribution of Plinian and sub-Plinian deposits of Somma-Vesuvius eruptions.

thermal system related to the magma chamber. This causes abrupt changes in the dynamics of the events, so triggering hydrothermo-phreatomagmatic processes that reinforce the explosive energy. In the A.D.79 eruption, the beginning of the caldera collapse is marked in fact by a "hydrothermo-magmatic" phase producing widespread turbulent pyroclastic flows and is followed by the emplacement of coarse, lithic-enriched debris flows, possibly from a multiple vent system. Similarly, in the Pomici di Base eruption, debris flow deposits and pyroclastic surges driven by hydrothermal-phreatomagmatic activity mark the syn-caldera phase.
The quiescence periods preceding the Plinian eruptions last from few centuries to millennia (Fig. 4).

Geophysics and subsurface information
Vesuvius is located at the intersection of NW-SE and NE-SW oriented fault systems. Deep drilling show that the shallow structure beneath the volcano comprises 1.5-2 km of inter-bedded lavas and volcaniclastic, marine, and fluvial sedimentary rocks of Pleistocene age, overlying a Mesozoic limestone basement the top of which is at 2.5-3 km of depth; xenoliths from this basement occur in the majority of the home pyroclastic depositional units (Fig. 3).The age of the oldest drilled volcanics rocks (1,350 m bsl), indicates that the volcanism in the Vesuvian area was active since at least 400 ka.
Seismic tomography provides further information about the shallow volcano structure (e.g., Capuano et al., 2003, and references therein). On the basis of a seismic velocity anomaly (high P wave velocity, V_p, and high V_p/V_S conversion, V_S being the S wave velocity) along the volcanic vertical axis (e.g., De Natale et al., 2004a, 2004b; Zollo et al., 1996), it has been hypothesized the presence of a high-rigidity body, centered beneath the crater, extending down to about 5 km of depth bsl and with a lateral extension of less than 1 km. The high-rigidity zone is endowed with high magnetization above 2 km of depth bsl (Fedi et al., 1998), which has been imputed to the existence of solidified magma (e.g., De Natale et al., 2004a, and reference therein). This is in agreement with the distribution of earthquake hypocenters concentrated along the crater axis down to 6 km of depth bsl, without significant gaps, although a lot of events clustered between 2 and 4 km bsl (Vilardo et al., 1999). Magnitude-frequency analysis shows that the physical conditions responsible of seismicity do not change within the seismogenetic volume. The seismicity is governed by a not-uniform stress acting within a pre-fractured medium. Furthermore, it is triggered by pore pressure variations related to the downward migration of hydrothermal fluids (Vilardo et al., 1999).
Seismic information about the deeper structure comes from reflected waves of active sources and from P-S converted waves of teleseisms. Such data point out that a rather large discontinuity, likely representing the top of a

magmatic sill, is located at about 10-15 km depth bsl. (Zollo et ali, 1996). A more refined active P and S wave reflection study (Auger et ali, 2001) identified a wide horizontal midcrustal magma sill, hosted in a densely fractured volume of rock, about 8 km deep, in agreement with magnetotelluric data showing the existence of low-resistivity levels at depths exceeding 8 km bsl (Di Maio et al., 1998). This depth coincides with the zone of clinopyroxene crystallization, as indicated by inclusion data (Belkin et al., 1985; Marianelli et al., 1995; 1999). The Moho discontinuity in the Vesuvius area is at a depth of 29-30 km (Piochi et al., 2004). The roots of the magma sill extend down to 30 km bsl, according to De Natale et al. (2001). Therefore such a layer is expected to represent the top of the feeding magmatic system. On the other hand, no clear reflection-conversion layer of significant extension is imaged at shallower depths.

Rock petrology and magma processes

Volcanic rocks produced at the Mount Somma-Vesuvius exhibit variable degrees of silica undersaturation and potassium enrichment and a large range of mineralogical, chemical and isotopic compositions (e.g., Piochi et al., 2006, Di Renzo et al., 2007 and references therein). Particularly, Mt. Somma-Vesuvius rocks span from shoshonite to trachy-phonolite, partially overlapping chemical composition of rocks produced at the Campi Flegrei area, and from alkalibasalt to tephrite and phonolite (Figs 4 and 11). The degree of silica undersaturation increases through time, and thus is highest in rocks of the last cycle and lowest in the rocks dated between 39 to about 19 ka bp. The products of the last period, from AD 79 to AD 1944, range from leucititic tephrite to leucititic phonolite. Based on petrographic descriptions (Rosi and Santacroce, 1983; Marianelli et al., 1999; Santacroce et al., 2007), slightly and mildly silica undersaturated rocks older than 472 AD contain phenocrysts and microlites of clinopyroxene, plagioclase, opaque Fe- and Ti-oxide minerals, biotite, and apatite, in order of decreasing abundance. Olivine is a phenocryst in the least evolved rocks; leucite microlites and microphenocrysts and K-feldspar phenocrysts appear in the most evolved rocks. Leucite is absent only in shoshonites to trachytes of the older magmatic period of volcanism. Nepheline is the only feldspathoid in the Pomici di Avellino rocks. Highly silica undersaturated rocks of the last volcanic period are generally strongly porphyritic with abundant clinopyroxene and leucite, opaque minerals, apatite and minor or rare plagioclase, biotite, and K-feldspar. Common accessory phases are scapolite, melanite, forsterite and amphibole. A wide range of Sr isotope compositions have been documented (Fig. 11), generally from ~0.7066 to ~0.7081 (e.g., Piochi et al., 2006, Di Renzo et al., 2007 and references therein). $^{143}Nd/^{144}Nd$ ratio ranges from 0.5126 to 0.5124; Pb isotope ratio show smaller ranges (e.g. of values for $\delta^{18}O$ (7.3-11.4‰) (Ayuso et

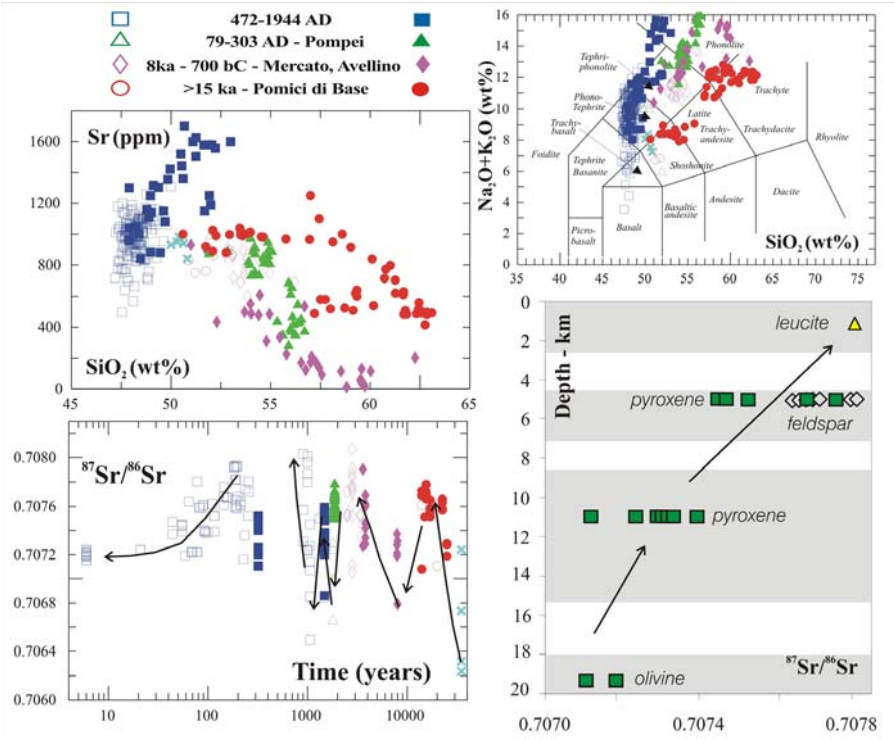

Figure 11. Whole-rocks chemistry and Sr-isotopes and relation between crystallization depth and $^{87}Sr/^{86}Sr$ of phenocrysts.

al., 1998 and references therein), whereas $^{3}He/^{4}He$ ratios are clustered around 2.4 R/Ra (Martelli et al., 2008). Strong isotopic disequilibria occur among minerals and between minerals, rocks and glass. The isotope and geochemical data for Plinian eruption products evidence that the magma chamber(s) feeding Plinian eruptions (3-5 km depth; Barberi et al., 1981) were generated by refilling and mingling of isotopically distinct, mafic, high-T (>1150°C) magma batches rising from deeper levels (Cioni et al., 1999 and references therein). Detailed petrochemical studies on plinian products from Pomici di Base (22 ka), Pomici di Avellino (3.8 ka), Pomici di Pompei (79 AD) and Pollena (472 AD) eruptions (e.g., Civetta and Santacroce, 1992) have suggested that the above processes produced a chemically and isotopically zoned shallow magma chamber (Fig. 12). On the contrary, during open conduit conditions the deep, volatile-rich magma batches rise to less than 2 km of depth and mix with the crystal-rich, volatile-poor resident magma (Fig. 13), triggering eruptions (Marianelli et al., 1999 and references therein).

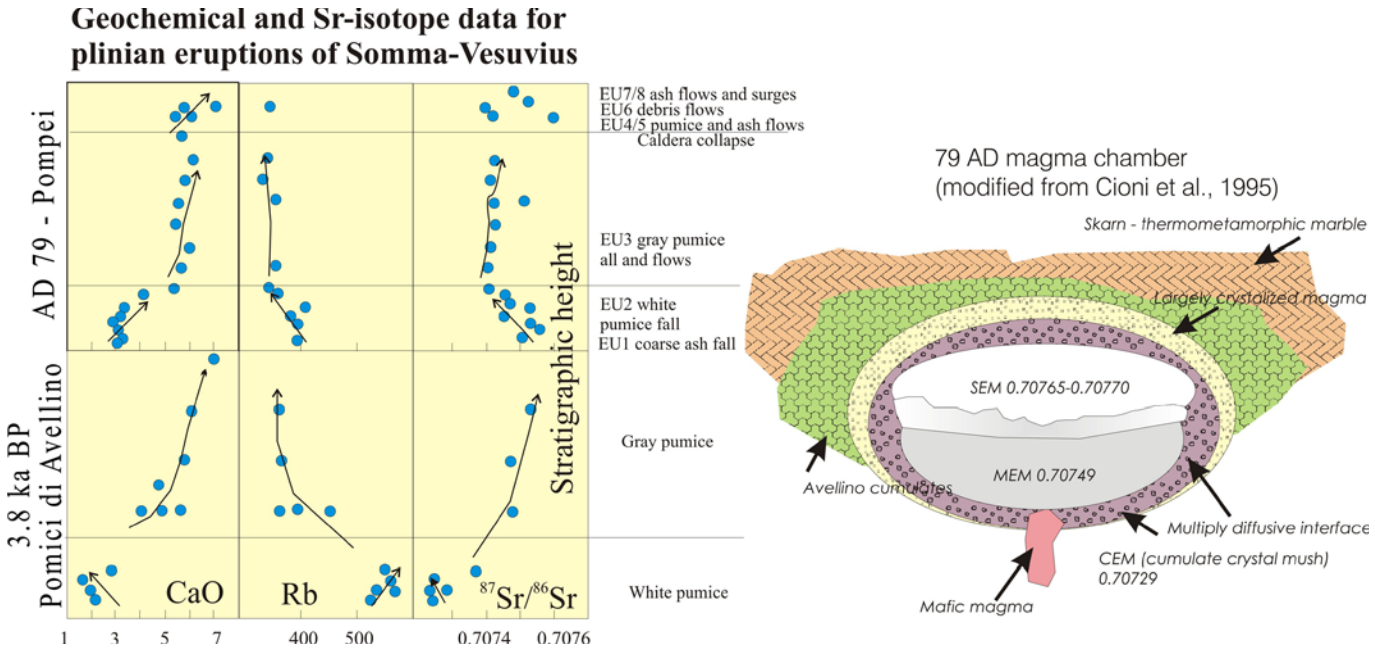

Fugure 12. Chemostratigraphy of two Plinian eruptions and sketch of the feeding magma chamber (After Cioni et al., 1995, and Civetta and Santacroce, 1992, and references therein).

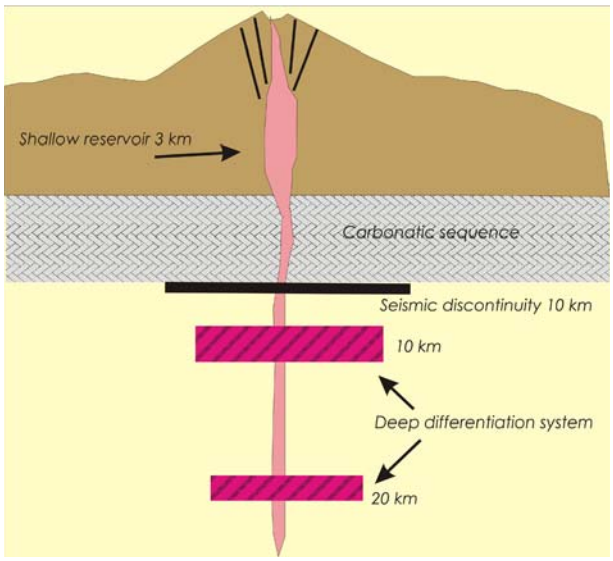

Figure 13. Sketch of the magmatic system feeding the 1944 eruption, with deep stratigraphic and seismic information (Auger et al., 2001; De Natale et al., 2004) (modified after Marianelli et al., 1999).

Genesis of the Vesuvian magmas is likely related to a source enriched by slab derived fluids or melts (Ayuso et al., 1998; Piochi et al., 2006; Santacroce, 1987, and references therein). Major and trace elements as well as isotopic trends indicate the existence of different magmatic reservoirs in which magma evolved (e.g., Ayuso et al., 1998; Civetta and Santacroce, 1992; Cortini Lima et al., 2003; Marianelli et al., 1999; Piochi et al., 2006). Pressure and temperature conditions and volatile concentrations of these reservoirs are inferred from melt and fluid inclusions trapped in phenocrysts through the analysis of dissolved volatiles. In particular, H_2O and CO_2 contents by means of Fourier transform infrared spectroscopy (FTIR) of inclusions in olivine and pyroxene phenocrysts (e.g., Belkin and De Vivo, 1993; Cioni, 2000; Lima et al., 2003; Marianelli et al., 1999) indicate at least two main different crystallization levels, respectively at depths of 3.5-5 km and deeper than 10 km bsl. Depending on the degree of differentiation, magmas in the chambers have temperatures between 1100 and 1500°K and dissolved volatile contents (H_2O/CO_2) between 2.5 and 6 wt %. The shallower chamber feeding Plinian eruptions has been located within the carbonatic platform (Barberi et al., 1981;), although no geophysical evidence confirms its existence at present. The relationship between Sr isotopic ratios and the equilibrium crystalliza-

tion depths of phenocrysts (Figs. 11 and 12) indicates that the deeper reservoir (~10 km) produces magmas with $^{87}Sr/^{86}Sr$ values lower than 0.7073, in contrast to the shallower one, in which most radiogenic magmas were generated, likely due to crustal contamination during magma evolution (Piochi et al., 2006). On the basis of Sr isotope, fluid inclusion and mineral chemistry data, the last 1944 eruption was fed directly by this deep reservoir, with magmas having a temperature of about 1500°K and dissolved volatile contents around 3 wt % (e.g., Belkin and De Vivo, 1993; Lima et al., 2003; Marianelli et al., 1999; Piochi et al., 2006). This eruption ended a continous period characterized by the ascent of magma batches from deeper levels, started after the last sub-plinian eruption. The highly Sr-isotopic variability detected in the produced rocks (Fig. 11) suggets that the higher Sr-isotopic ratios have been acquired at a shallower depth likely by crustal contamination during magma evolution. In contrast the lower Sr-isotope compositions characterise the less contaminated magmas coming from deeper crustal levels. Therefore, the temporal Sr-isotopical variation of magmas erupted in the 1631-1944 AD period probably derives from the progressive withdrawal of the shallow magma chamber, which was completely empty before the 1805-1944 AD period of volcanism. Therefore the effusive and explosive events of the most recent 1805-1944 AD period were fed directly by the deep reservoir located at depth exceding 11km (Fig. 13).

Features of fluids at the surface

Since 1944 to 1960 temperatures between 900 and 1100°K were measured in the crater area, whereas temperatures decreased in the period afterward (Chiodini et al., 2001). Mineralogical changes of fumarolic sublimates collected since 1944 suggest that magmatic gases were discharged during the initial ‘‘hot’’ period following the last eruption (Chiodini et al., 2001). Although data on magmatic gases discharged at that time are lacking, their composition can be inferred from melt inclusions (MI) in the products of the last eruption; based on data from Marianelli et al. (1999), a molar concentration ratio X_{CO2}/X_{H2O} of about 2.7 in the gas phase can be estimated. Petrological data (e.g., Lima et al., 2003) indicate that dissolved S-, Cl-, and F-bearing species are subordinated to H_2O and CO_2. This applies also to exsolved gaseous species, so that the heat transfer in the volcanic edifice due to degassing can be properly related to the flux of water and carbon dioxide. High Cl content of 1944 magma supports the geochemical model of Chiodini et al. (2001) about the hydrothermal system beneath the volcano. In this model, Cl-rich brines, fed by magmatic gases, developed at P-T conditions very close to their critical point and in a high-temperature reservoir (between 640 and 720°K). The chemical composition of gases (SO_2, HCl, HF, particularly) presently discharged by the fumaroles at the crater bottom is therefore

buffered by such a saline hydrothermal system (Chiodini et al., 2001). Although thermo-metamorphic reequilibration is attained between the Cl-rich hot brine and the surrounding carbonates (Chiodini et al., 2001), Federico et al. (2002) show that the isotopic ratio of helium and carbon dissolved in Vesuvian groundwaters have the magmatic signature (Martelli et al., 2008). Similarly, He isotope ratios from gas fumaroles at the crater are in the range of values detected in olivine phenocrysts (Martelli et al., 2008). Diffuse degassing survey of soil CO_2 flux performed at Mount Vesuvius reveals that about 150 tons per day of deeply derived CO_2 are released by the volcanic apparatus just around the crater axis. Chiodini et al. (2001) suggest that no input of fresh magma at shallow depths took place after 1944 A.D., so that such a CO_2 mass rate may be taken as a constant after the last eruption.

DESCRIPTION OF STOPS (LOCATION IN FIG. 1)

Stop 1
The AD 79 eruption at Oplonti excavations

The AD 79 "Pompeii" eruption. On August 24 of AD 79, Vesuvius awakened and destroyed the towns of Herculaneum, Oplontis, Pompeii and Stabiae. The eruption has been studied by many authors (Lirer et al., 1973; Sigurdsson et al., 1985; Barberi et al., 1989; Cioni et al., 1999; Gurioli et al., 2002; 2007) and three major phases have been distinguished: (1) opening phreatomagmatic; (2) main Plinian; (3) caldera-forming with phreatomagmatic surges and flows emplacement. The AD 79 eruption sequence includes 8 Eruption Units, each with distinct sedimentological characteristics, areal distribution and lateral variations, emplaced by pulses within a phase, with well defined eruptive mechanism (Figs. 14 and 15).
An accretionary lapilli-rich ash layer (EU1), the only product of the opening phreatomagmatic phase, is covered by the pumice-fall deposit of the Plinian phase. This latter phase was dominated by an eruption column which reached a maximum altitude of 30 km. The Plinian deposit is composed of white phonolitic pumice (EU2F), locally capped by a thin, whitish ash-flow deposit (EU2/3PF), which passes upwards, with a sharp colour change, to grey, mafic phonolitic pumice (EU3F). The upper part of the deposit contains intercalated ash-flow beds (EU3PF); in proximal exposures, the sequence ends with pumice and ash-flow deposits. During this phase, which tapped more than 3 km^3 of magma, thick fallout deposits accumulated on a large area to the southeast, and pyroclastic-current deposits buried Herculaneum to the south. The caldera forming phase began with the most powerful and widespread pyroclastic current (EU4) deposition and continued with the emplacement of

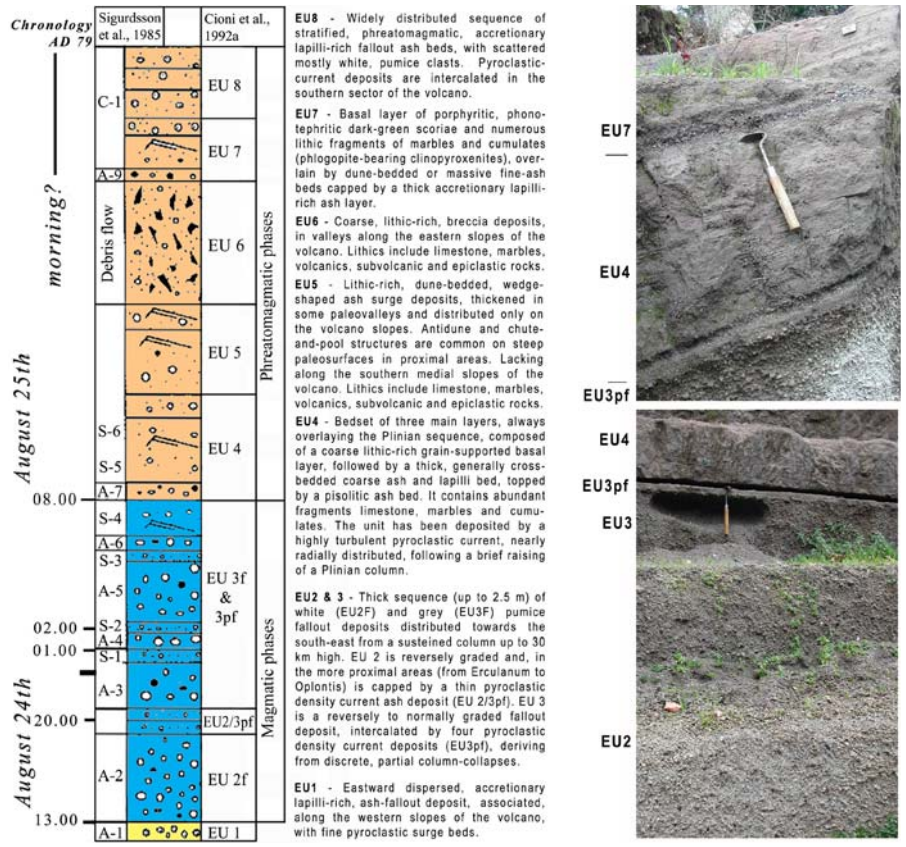

Figure 14. Generalised sequence of the AD 79 Vesuvius eruption deposits.

the pyroclastic-current deposits of EU5. The strong earthquake and the dark cloud witnessed by Pliny the Younger at Cape Misenum on the morning of August 25 likely correspond to the EU4 pyroclastic current. These currents destroyed human settlements along the western and northern slopes of the volcano and devastated the Pompei-Stabia area. EU5, distributed in proxi-mal areas and confined in valleys of the volcanic edifice, is covered by very coarse, lithic breccia flow deposits of EU6, extensively exposed along the eastern slopes of Mt. Somma.

Areal distribution as well as lithic types and content of the latter deposits, suggest that they were erupted during the paroxistic events of the caldera-forming phase. The protracted withdrawal of the magma chamber, favoured by magma-water interaction, led to tapping of the more mafic liquid that

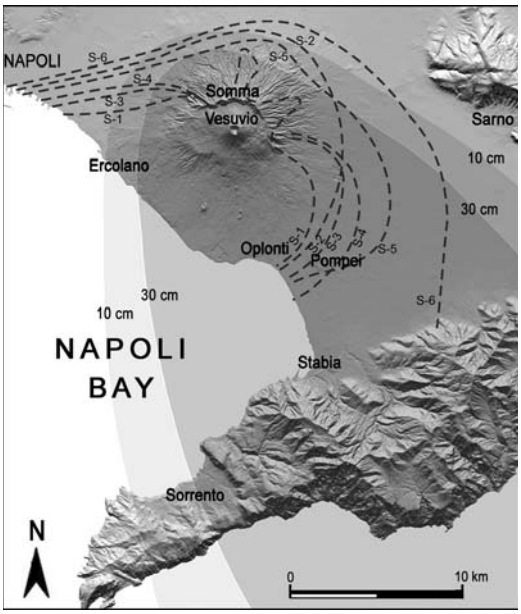

Figure 15. Areal distribution of the AD 79 Vesuvius eruption deposits. Shaded areas: fallout deposits; dashed lines: surge deposits (after Sigurdsson et al., 1985).

characterizes the juvenile fraction of the widespread EU7. During the waning stage of the eruption, wet, phreatomagmatic, ashy pyroclastic currents (EU8) were generated, showing a sharp compositional reversal towards the more salic compositions of the initial phase of the eruption.
The Plinian deposits (fall and minor flows) range from early phonolitic white pumice to late tephritic-phonolitic grey pumice (Fig. 12); the upper phreatomagmatic flow units exhibit larger variations with both grey and white pumice clasts and more abundant mafic crystals in the grey pumice. White pumice results from the withdrawal of phonolitic magma from the top of the chamber. Magma temperature was evaluated at about 850-900° on the basis of homogenisation temperature of glass inclusions within sanidine and leucite (Cioni, 2000). The grey pumice results from the mixing of three isotopically distinct components: phonolitic white melt, mafic cumulates and a crystal-poor grey magma. The grey magma had high temperature (around 1050° C), very low viscosity and density slightly higher than that of the white magma. These features are consistent with the establishment of a physical discontinuity separating the white from the grey body. The lower portion of the Pompeii chamber was therefore occupied by a homogeneous, phonolitic-

tephritic, grey magma which was never erupted without being largely mixed. The grey-white mixing was mainly sin-eruptive, as suggested by variations in magma discharge rate closely linked to the extent of the mixing.

Oplontis, Villa di Poppea. Villa di Poppea, at Oplontis, is a wonderful excavation of a luxurious Roman Villa, probably owned to Poppea, imperator Nero's wife. The Villa was buried by the deposits of 79 AD eruption, as it situated on the western side of the dispersal fan of the fallout deposits. In this site it is possible to look an almost complete sequence of deposits of the AD 79 eruption, composed by fallout and pyroclastic density current deposits, interlayered with and overlying the fallout sequence (Fig. 16).
The gray fallout bed of the EU3 is interrupted by 4 ash deposits that Sigurdsson et al (1985) related with partial column collapses of the sustained column. This interlayering characterizes only the medial deposits of the southern sector. The white - gray pumice interface does not contain here the first generated pyroclastic density current deposit, exposed in other proximal outcrops.

Fig. 16. Sequence of deposits of the AD 79 eruption at Oplontis.

At the top of the plinian fallout and flow sequence, it is possible to observe the EU4 deposits, formed by a fining upward deposit with a coarse, dune-bedded lower portion followed by a massive upper layer. The sequence is closed by the wet deposits of the final phreatomagmatic phase, and by flood deposits which affected a wide territory around the volcano for a long time.

Stop 2

The Piano delle Ginestre, the western part of the Monte Somma caldera

The Somma-Vesuvius caldera is a poly-phased structure whose evolution has been newly approached by studying the pyroclastic successions of the last 22,000 years of the volcano's history (Cioni et al., 1999). The remnants of the summit caldera are well identifiable with the northern inner walls of Mt Somma, formed by some curved lineaments partially withdrawn by subsequent slope failures.

Coalescent and nested structures, derived from several collapses, have been identified. In particolar, four main collapse episodes occurred during the more energetic Plinian eruptions: at ~22 ka (Pomici di Base), 8.8 ka (Pomici di Mercato), 3.8 ka (Pomici di Avellino) and in AD 79 (Pomici di Pompei) (Figs. 5 and 17). Further minor caldera collapses probably associated with some lower magnitude eruptions, such as those at 472 or 1631 A.D. The collapsed areas are not exposed, probably because the caldera occurred inside a preexisting structure, and the depression was subsequently buried or renewed. This is the case of the 1631 caldera, which was followed by a collapse of the area now approximately occupied by the Vesuvius cone.

The presence of a large wedge of syn-caldera breccias, up to 80 m thick, in the north-west sector of Somma, clearly indicates that the quasi-vertical wall running from the Fosso della Vetrana to Cognoli di Trocchia is the remnant of a summit eccentric collapse related to the 22 ka Pomici di Base Plinian eruption. The position of very proximal fallout deposits of the first phase of the eruption suggests that the vent was not centered on the present conduit area.

The central sector of the caldera wall, facing the Valle dell'Inferno, has been dubiously related by Cioni et al. (1999) to the 8,8 ka Pomici di Mercato eruption. This segment of the caldera wall is formed by at least two main arcs, affected by landslides that have partly withdrawn the original scarp of the caldera. The very thick, lithic rich pyroclastic flows, present on the northern slopes of the volcano, just outside the main remnants of the caldera walls, were emplaced in the final stages of the this eruption, likely during the caldera collapse (more than 1 km^3 DRE).

The pronounced lobe which characterizes the western slopes of the Somma caldera is named Piano delle Ginestre (Fig. 1). This elliptic structure is delimited to the north by the crescent-shaped Observatory Hill relief, while its south-

Figure 17. Idealized reconstruction of the morphology of Somma-Vesuvius after each caldera collapse.

western flank is formed by a wedge of pyroclastic deposits. This later is mostly related to the Pomici di Avellino and Pomici di Pompei eruptions, which formed a rampart lying on the old edifice. The Piano delle Ginestre has been interpreted as a complex, constructive-destructive structure, nested in the Pomici di Base caldera and formed during the 3.8 ka Pomici di Avellino Plinian eruption. The thick pyroclastic surge deposits emplaced in the final phases of the eruption contributed to build the Piano delle Ginestre rim, just outside the vent area. This ring-shaped depression was subsequently filled by the effusive and pyroclastic products of the following eruptions. After the filling of the depression, lava flows poured toward the sea from a notch in the western rim of the structure.

The southern and south-eastern portions of the present caldera depression are linked to the A.D. 79 eruption.

The reconstruction of the caldera evolution involves a migration of the vent position. Both the Pomici di Base and Pomici di Avellino are related to eruptive vents located on the western flank of the volcano. The shape and position of the Pomici di Pompei caldera suggests that the eruptive vent was probably located in the southern part of the present caldera depression.

In this stop the main features and evolution of the caldera in relation with the magmatic feeding system withdrawal will be discussed. Along Piano delle Ginestre we will see also variable types of lavas including the lavas emitted during the first two days of the 1944 eruption.

Stop 3
The present Crater and the 1944 eruption of Vesuvius

The 1944 eruption is the last event of Vesuvius (Fig. 4). Since then, the volcano is quiescent, only fumaroles and moderate seismicity testify its activity. The 1944 eruption closed a cycle of persistent activity, begun in 1914 and characterised by mainly effusive central eruptions which completely filled the 1906 pre-existing crater (720 m wide and 600 m deep) (Figs. 18 and 19). 50-100 millions of m^3 of lavas and pyroclasts have been emitted in this time span. A description of the eruption was reported by Imbò (1949) and here summarised.

On March 13, the spatter cone, emerging from the crater (Fig. 19), began to collapse and seismicity increased. A new cone formed between March 13 and 16 and collapsed on March 17.

The eruption begun on the afternoon of March 18 with Strombolian activity. A lava flow overflowed the northern portion of the crater rim at 4.30 pm, and reached the Valle dell'Inferno at 10.30 pm (Fig. 20).

Other lavas overflowed the southern portion of the rim, almost contemporaneously, and the western portion at 11.00 pm, reaching the Fosso della Vetrana at 11.00 am of March 19. From the afternoon of March 20 and for the following night, new lava flows overflowed the northern portion of the crater rim. On March 21, the southern lava flow stopped at about 300 m a.s.l., while the northern flow reached the towns of S. Sebastiano al Vesuvio and Massa di Somma between 1.00 and 2.00 am. The 10,000 inhabitants were evacuated and transferred to Portici. Around 5.00 pm a new phase of the eruption

Figure 18. View of the crater after the 1906 eruption (after Diario del Monte Vesuvio by GP Ricciardi).

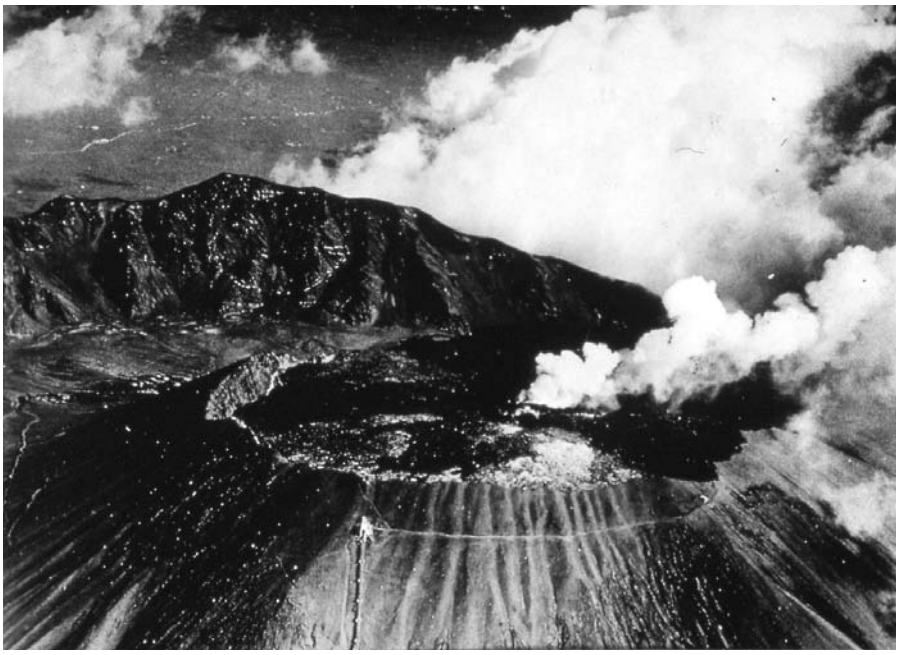

Figure 19. View of the 1906 crater completely filled by the 1914-1944 intracreteric effusive and explosive activity. Note the small smoking spatter cone just at the center of the crater and the not jet destroyed Funicolare (after Diario del Monte Vesuvio by GP Ricciardi).

which generated 8 spectacular lava fountains, began and lasted till 00.48 pm of the next day. The last fountain, lasted about 5 hours, reached an height of about 1,000 m. Scoriae and ash fallout beds were laid down southeast of the volcano, between the towns of Angri and Pagani. Large amount of incandescent scoriae, due to the ground movements related to intense seismic tremor, generated hot avalanches which reached the foot of the cone.
At 00.48 pm of March 22 there was a transition from the lava fountains phase to a buoyant column phase (Fig. 21). The convective portion of this column, 5-6 km high, was dispersed towards the southeast. Partial collapses generated pyroclastic currents which moved along the slopes of the cone. This eruption phase, during which the crater enlarged progressively, was characterised by intense seismic tremor. On March 23 a new and last phase began. It was dominated by phreatomagmatic explosions with energy decreasing through time. Also seismicity changed from tremor to discrete shocks. The ash-rich columns were directed towards the south-south-west, and small pyroclastic

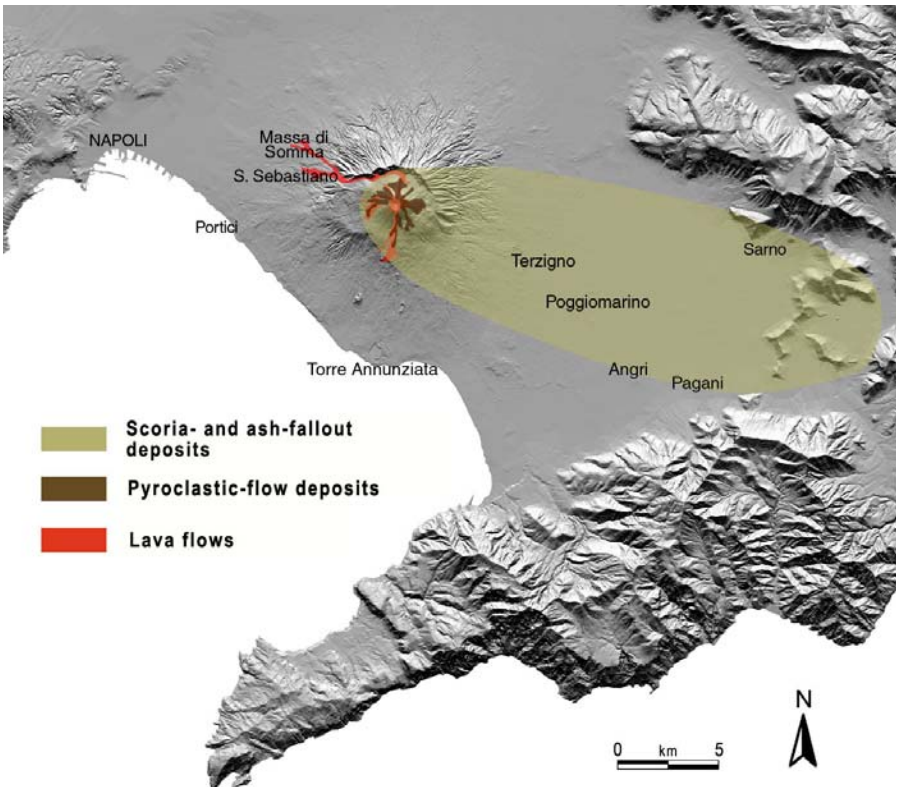

Figure 20. Distribution of the 1944 Vesuvius eruption deposits.

currents flowed on the slopes of the cone (Fig. 21). The eruption ended on March 29.

The 1944 products range in composition from phonolitic tephrite to tephrite, resulting from mixing between variable magma batches and crystals (Marianelli et al., 1999). K-phonotephrites were produced during the effusive phase and the first lava fountain, whereas the emission of strongly porphyritic K-tephrites took place during the more intense fountain. The lower portion of the pyroclastic sequence includes both brownish vesicular and dark dense lapilli juvenile clasts. The two types of clasts, petrographically and chemically similar, differ for vesicularity, matrix colour (yellowish to brownish) and crystallinity. The upper portion of the sequence includes only denser juvenile clasts, richer in clinopyroxene and leucite.

Phenocrysts content increases and vesicularity decreases up-section. Clinopyroxene is ubiquitous phenocryst phase and occurs in two varieties, a

Figure 21. Buoyant column phase of the 1944 Vesuvius eruption.

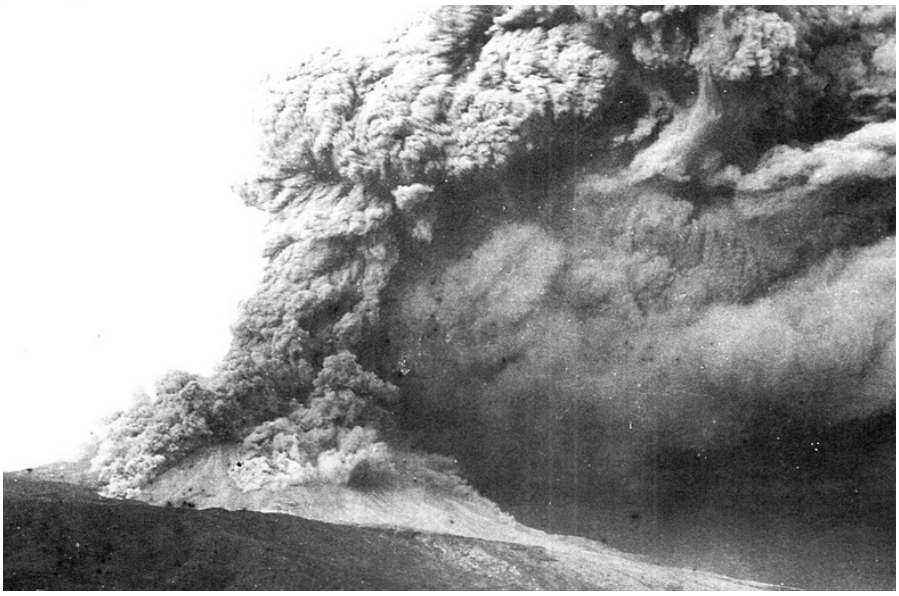

Figure 22. Partial column collapse with generation of pyroclastic currents during the last phases of the 1944 Vesuvius eruption.

colourless diopside and a greenish salite. Leucite, plagioclase, biotite and olivine occur as phenocrysts and in glassy groundmass along the all sequence, in different proportion. In particular, leucite is widespread at the base and clinopyroxene and olivine occur as loose megacrysts in the upper part of the sequence.
Melt inclusions compositions (major and volatile elements) highlight that the erupted magmas underwent differentiation at different pressures. The K-tephritic volatile-rich magma (up to 3 wt.% of H_2O, 3.000 ppm of CO_2 and 0.55wt. % of Cl) evolved to a K-phonotephritic melt through crystallization of diopside and forsteritic olivine at total fluid pressure >300 (up to 600, Marianelli et al., 1999) MPa. This magma fed a very shallow reservoir (Fig. 13). The low pressure differentiation of the volatile-poor K-phonotephritic magmas (H_2O <1 wt.%) involved mixing, open-system degassing, and crystallization of dominant leucite, salite, and plagioclase. The eruption was triggered by intrusion of a volatile-rich magma rising from a depth of 11-22 km into the shallow (1.5 km) magma chamber. The lava effusion phase of the eruption partially empted the shallow reservoir, the top of which is within the caldera edifice. The newly arrived magma mixed with that resident in the shallow reservoir and forced the transition to the lava fountain phase.
The pyroclastic deposits also contain lithics of skarn and other thermo-metamorphic rocks, grouped in four main litho-types: metasomatised cumulites, Ca-skarn, Mg-skarn and cornubianites. These rocks, which could result from interaction between magma and magma chamber sedimentary wall-rocks (limestones, dolomites, marls and siltites), are peculiar of the 1944 eruption. It is has been suggested that the magma chamber was a high aspect ratio structure, reaching the sedimentary basement of the volcano around 3-4 km of depth. The presence of periclase in the Mg-Skarn could suggest hypo-abyssal conditions with maximum pressures of 1,000 bars.
The most relevant effects of the eruption are: twenty-six people dead in the area affected by lapilli and ash fallout, due to roofs collapse; two villages partially destroyed by lava flows; three years of missed crops in the downwind area.

The crater. A complete sequence of the 1914-1944 deposits of the last cycle of activity at Vesuvius is exposed along the north-eastern portion of the crater slope (Fig. 23). The sequence is dominated by lavas, the most significant was extruded on 1929, with minor spatter and scoriae beds. It is horizontal, fills the 1906 eruption crater and unconformably covers the pre-existing sequence of rocks exposed in the 1906 crater. Both sequences are topped by the deposits of the 1944 eruption. Their base is a grey massive lava, the first unit of the 1944 eruption sequence (Fig. 24), grading into a

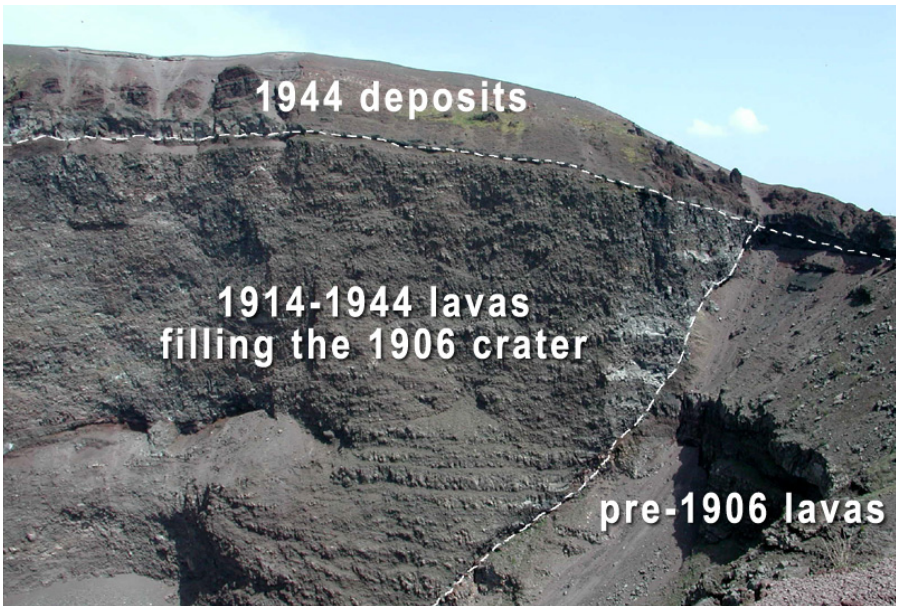

Figure 23. View of the north-eastern portion of the Vesuvius crater wall.

densely-welded crudely-stratified spatter succession emplaced during the lava fountaining phase.
The largest part of this succession was emplaced during the VIII fountain (7.30 am -00.48 pm, March 22), when concomitance of rapid spatters accumulation and strong seismic tremor, caused hot avalanches. The spatter succession is covered by another succession of black and grey scoriaceous lapilli and bombs deposits with interlayered coarse ash beds emplaced during the formation of the buoyant ash column. The upper part of the 1944 sequence includes a sequence of reddish and violaceous lapilli and bombs deposits, and coarse ash beds, and is topped by grey ash deposits rich in lithic fragments, mainly composed of fresh and hornfelsed lavas. It was deposited during the phreatomagmatic final phase of the eruption.

The Vesuvius fumaroles. Fumarols occur along the inner crater wall and within the crater floor. Those of the crater rim and inner slopes discharge fluids rich in atmospheric gases with outlet temperatures ranging from 60 to 75°C; those of the crater bottom have temperature close to the water boiling point since 1988. The H_2O is the a major constituent, followed by CO_2, H_2, H_2S, N_2, CH_4, and CO in order of decreasing concentrations, and undetectable SO_2, HCl, and HF.

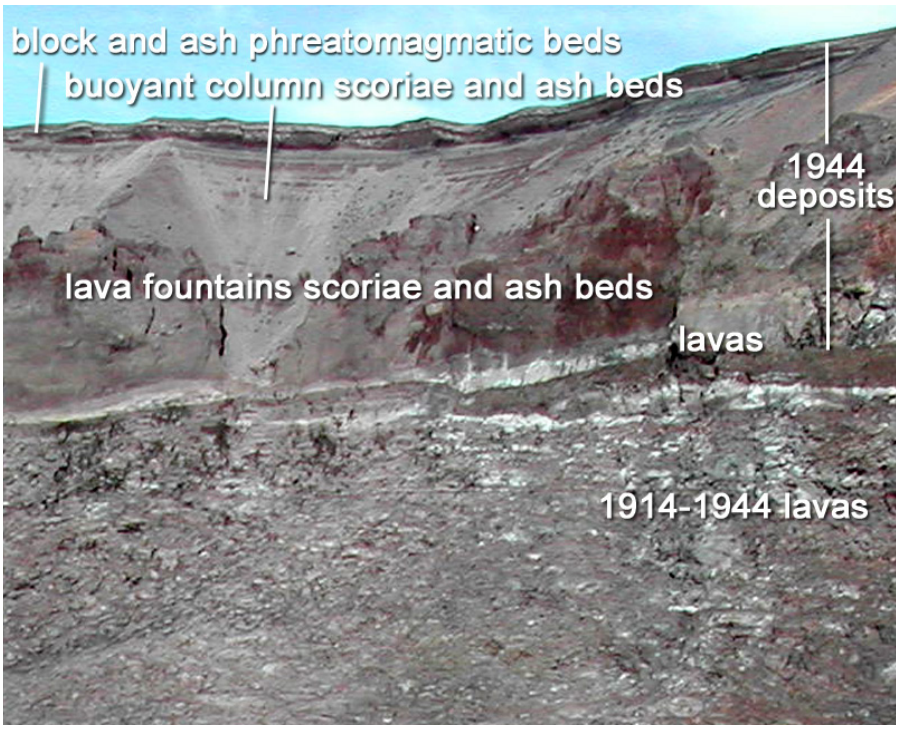

Figure 24. The 1944 Vesuvius eruption deposits along the northern crater wall.

Fumarolic water is either meteoric water enriched in ^{18}O through water-rock oxygen isotope exchange in the hydrothermal environment or a mixture of meteoric and arc-type magmatic water, as indicated by the $^{18}O_{H2O}$ values, suitably corrected for oxygen isotope exchange between H_2O and CO_2, and the D_{H2O} values. It is equally possible that both water-rock oxygen isotope exchange and addition of magmatic water take place in the hydrothermal system of Vesuvio crater. The hydrothermal component is higher in the crater bottom fumaroles.

Fumarolic CO_2 has a double origin: part of the CO_2 is of deep provenance (magmatic), and part is from metamorphic reactions involving marine carbonates (although addition of a small fraction of magmatic CO_2 cannot be ruled out), as suggested by both the $^{13}C_{CO2}$ values and gas equilibria. The decarbonation reactions results from a local thermal anomaly in the thick carbonate sequence, at >2.5 km underneath the volcano (Chiodini et. al., 2001). CO_2 is mainly fluxed by soil diffusion; its output is estimated at about 150 td^{-1}.

Stop 4

The Osservatorio Vesuviano historical building - information centre on volcanic hazards and risk

The Osservatorio Vesuviano, the oldest volcano observatory in the world, was founded in 1841 by the Bourbon King of two Sicilies, Ferdinand II. It was inaugurated during the 7th Congress of the Italian Scientists, held in Naples in 1845.

The historical site of the observatory (Fig. 25) is an elegant neo-classical building designed by the architect Gaetano Fazzini and strategically located on the Salvatore hill, at an elevation of 608 m a.s.l. It presently hosts a museum and two permanent exhibitions ("Vesuvius: *2,000 years of observations*" and "Vulcanica", *an itinerary through the world of volcanoes*) in which the visitors are introduced to volcanism and related hazards, the monitoring systems of active volcanoes (Fig. 26), and the history of Mt. Vesuvius and its Observatory and of the others active Italian volcanoes. The exhibitions are visited by a public of about 16,000 people per year, mainly composed of students from both Italy and other countries.

The position of the building was particularly favourable since the site, hosting already a small church and a hermitage dating back to 1600, had never been damaged by the very frequent eruptions, occurred after the large 1631

Fig. 25. Historical building of the Osservatorio Vesuviano

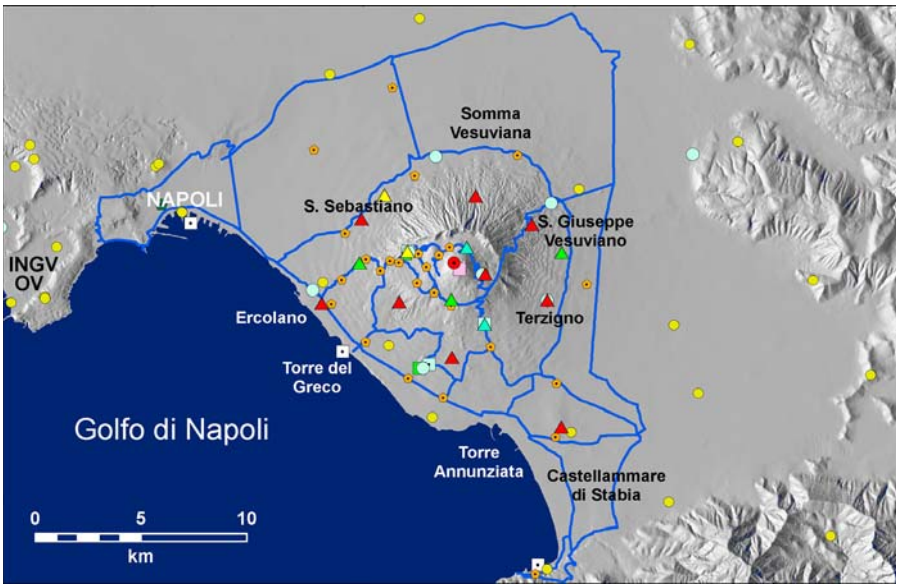

Fig. 26. Surveillance network of Vesuvius and Campi Flegrei volcanoes. Seismic station = triangle; tiltmeter= blue squre; gravimetric station= green pentagon; gravimetric benchmark= yellow pentagon; marigraphs= white square; infrared camera= red circle; geochemical station= pink square; dilatometer= green square; GPS station= blue circle; GPS benchmark= yellow circle; levelling network= blu lines.

event. The first director was Macedonio Melloni, one of the most prominent experimental physicists. The construction was completed in 1848; only a few months later, for political reasons, Macedonio Melloni was dismissed as director. His successor was the physicist Luigi Palmieri, at the time professor of philosophy at the University of Naples, who provided the Osservatorio with a meteorological tower. Luigi Palmieri built the first electromagnetic seismograph, with which he wanted to "make the smallest motions of the ground clear, recording them on the paper or indicating their nature, strength and duration". He first detected harmonic tremor caused by magma oscillation and degassing in the conduit and concluded that such a phenomenon could be used to forecast an eruption. The following directors were Raffaele Vittorio Matteucci and Giuseppe Mercalli. The latter, inventor of the homonymous scale of seismic intensity, drew the first modern classification of volcanic eruptions. Ciro Chistoni and Alessandro Malladra followed Mercalli in the director position. In 1937 Giuseppe Imbò was appointed as director. He strengthened the existing instruments on the volcano reaffirming the old objectives of Melloni and Palmieri of forecasting eruptions. He made instru-

ments for seismological, electrical and radioactive observations, carried on, hoping to forecast the final eruption of the cycle begun in 1913. Imbò with the aid of a seismograph and observations on the Vesuvius activity, managed to forecast the 1944 eruption and to inform the authorities. He was director until 1970, the year of the first ascending phase of the recent Phlegraean bradyseismic events.

REFERENCES

Andronico D, Cioni R (2001). *Contrasting styles of Mount Vesuvius activity in the period between the Avellino and Pompeii Plinian eruptions, and some implications for assessment of future hazards.* Bull Volcanol 64, 372-391.

Arrighi, S., Principe C., Rosi M. (2001), Violent Strombolian and subplinian eruptions at Vesuvius during post-1631 activity, Bull. Volcanol., 63, 126-150.

Auger, M., Gasparini P., Virieux J., Zollo A. (2001), Seismic evidence of an extended magmatic sill under Mt. Vesuvius, Science, 294, 1510-1512.

Ayuso R.A., De Vivo B., Rolandi G., Seal II R.R., Paone A. (1998), Geochemical and isotopic (Nd-Pb-Sr-O) variations bearing on the genesis of volcanic rocks from Vesuvius, Italy, J. Volcanol. Geotherm. Res., 82, 53-78.

Barberi F., Cioni R., Rosi M., Santacroce R., Sbrana A., Vecci R. (1989), Magmatic and phreatomagmatic phases in explosive eruptions of Vesuvius as deduced by grain-size and compositional analysis of pyroclastic deposits. J. Volcanol. Geotherm. Res, 38, 287-307.

Barberi, F., Leoni L. (1980), Metamorphic carbonate ejecta from Vesuvius Plinian eruptions: Evidence of the occurrence of shallow magma chambers, Bull. Volcanol., 43, 108-120.

Belkin, H. E., De Vivo B. (1993), Fluid inclusion studies of ejected nodules from Plinian eruptions of Mt. Somma-Vesuvius, J. Volcanol. Geotherm. Res., 58, 98-100.

Capuano P., Gasparini, P. Zollo A., Virieux J., Casale R., Yeroyanni M. (2003), The Internal Structure of Mt. Vesuvius. A Seismic Tomography Investigations, 595 pp., Liguori, Naples, Italy

Chiodini, G., Marini L., Russo M. (2001), Geochemical evidence for the existence of high-temperature hydrothermal brines at Vesuvio volcano, Italy, Geochim. Cosmochim. Acta, 65, 2129-2147.

Cioni, R. (2000), Volatile content and degassing processes in the A.D. 79 magma chamber at Vesuvius (Italy), Contrib. Mineral. Petrol., 140, 40-54.

Cioni R., Civetta L., D'Antonio M., de Vita S., Di Vito M., Fisher R.V., Marianelli P., Marinoni L., Orsi G., Ort M., Pappalardo L., Piochi M., Rosi M., Santacroce R., Sbrana A. (1995), *Volcanoes of the Neapolitan Area: Vesuvio and Campi Flegrei*, Guide-book to the field excursions, 1-3 Oct. 1995. Volcanoes in Town, a IAVCEI Conference on Volcanic Hazard in Densely Populated Regions.

Cioni, R., Longo A., Macedonio G., Santacroce R., Sbrana A., Sulpizio R., Andronico D., 2003. Assessing pyroclastic fall hazard through field data and numerical simulations: Example from Vesuvius. J. Geophys. Res. 108 (B2), doi:10.1029/2001JB000642, 2003.

Cioni, R., Santacroce R. Sbrana A. (1999), Pyroclastic deposits as a guide for reconstructing the multi-stage evolution of the Somma-Vesuvius caldera. Bull. Volcanol., 60, 207-222.

Civetta, L., Santacroce R. (1992), Steady state magma supply in the last 3400 years of Vesuvius activity. Acta Vulcanologica, Pisa 2, 147-159.

D'Argenio, B., Pescatore T., Scandone P. (1973), Schema Geologico dell'Appennino Meridionale (Campania e Lucania), paper presented at Moderne Vedute Della Geologia dell'Appennino, Accad. Naz. dei Lincei, Rome.

De Natale G., Kuznetzov I., Kronrod T., Peresan A., Sarao` A., Troise C., Panza G. F. (2004a), Three decades of seismic activity at Mt. Vesuvius: 1972-2000, Pure Appl. Geophys., 161, 123-144.

De Natale G., Troise C., Pingue F., De Gori P., Chiarabba C. (2001), Structure and dynamics of the Somma-Vesuvius volcanic complex, Mineral. Petrol., 73(1- 3), 5-22.
De Natale G., Troise C., Trigila R., Dolfi D., Chiarabba C. (2004b), Seismicity and 3-D substructure at Somma-Vesuvius volcano: Evidence for magma quenching, Earth Planet. Sci. Lett., 221, 181-196.
de Vita S., Sansivero F., Orsi G., Marotta E., Piochi M., 2010. Volcanological and structural evolution of the Ischia resurgent caldera (Italy) over the past 10 ka. Geological Society of America, Special Paper, 464, 193-239
Di Maio R., Mauriello P., Patella D., Petrillo Z., Piscitelli S., Siniscalchi A. (1998), Electric and electromagnetic outline of the Mount Somma-Vesuvius structural setting, J. Volcanol. Geotherm. Res., 82, 219-238.
Di Renzo, V., Di Vito M.A., Arienzo I., Carandente A., Civetta L., D'Antonio M., Giordano F., Orsi G., Tonarini S. (2007), Magmatic history of Somma-Vesuvius on the basis of new geochemical and isotopic data from a deep borehole (Camaldoli della Torre). J. Petrol., 48, 753-784, doi:10.1093/petrology/egl081.
Di Vito M. A., Isaia R., Orsi G., Southon J., D'Antonio M., de Vita S., Pappalardo L., Piochi M., 1999. *Volcanism and deformation since 12,000 years at the Campi Flegrei caldera (Italy)*. J. Volcanol. Geotherm. Res., 91, 221-246.
Di Vito, M.A, Zanella E., Gurioli L., Lanza R., Sulpizio R., Bishop B., Tema E., Boenzi B., Laforgia E., (2009) The Afragola settlement near Vesuvius, Italy: The destruction and abandonment of a Bronze Age village revealed by archaeology, volcanology. Earth Planet. Sci. Lett., 277 (2009) 408-421.
Di Vito, M.A., Sulpizio R, Zanchetta G., D'Orazio M. (2008), The late Pleistocene pyroclastic deposits of the Campanian Plain: New insights into the explosive activity of Neapolitan volcanoes. J. Volcanol. Geotherm. Res., 177, 19-48.
Doglioni, C. (1991), A proposal for kinematic modeling of W-dipping subductions: Possible applications to the Tyrrhenian-Apennines system, Terra Nova, 3, 426- 434.
Fedi M., Florio G., Rapolla A. (1998), 2.5D modelling of Somma-Vesuvius structure by aeromagnetic data, J. Volcanol. Geotherm. Res., 82, 239-247.
Gurioli L., Sulpizio R., Cioni R., Sbrana A., Santacroce R., Luperini W., Andronico D. (2010) Pyroclastic flow hazard assessment at Somma-Vesuvius based on the geological record. Bull Volcanol 72:1021-1038
Gurioli L., Cioni R., Sbrana A., Zanella E. (2002), Transport and deposition from pyroclastic flows over densely inhabited areas: Herculaneum (Italy). Sedimentology, 46, 1-26.
Gurioli L., Zanella E., Pareschi M. T., Lanza R. (2007), Influences of urban fabric on pyroclastic density currents at Pompeii (Italy): 1. Flow direction and deposition, J. Geophys. Res., 112, B05213, doi:10.1029/2006JB004444.
Imbò G. (1949), L'attività vesuviana e relative osservazioni nel corso dell'intervallo eruttivo 1906-1944 ed in particolare del parossismo del marzo 1944, Ann Osservatorio Vesuviano Serie V, 185-380.
Johnston Lavis, H.J. (1884), The geology of the Mt. Somma and Vesuvius: being a study of volcanology. Q J Geol Soc Lond, 40, 35-149.
Lima, A., Danyushevsky L.V., De Vivo B., Fedele L. (2003), A model for the evolution of the Mt. Somma-Vesuvius magmatic system based on fluid and melt inclusion investigations, in Melt Inclusions in Volcanic Systems: Methods, Applications and Problems, edited by B. De Vivo and R. J. Bodnar, pp. 227-249, Elsevier, New York.
Lirer L., Pescatore T., Booth B., Walker G.P.L. (1973), Two Plinian pumice-fall deposits from Somma-Vesuvius, Italy. Geol. Soc. Am. Bull., 84, 759-772.
Marianelli, P., Metrich N., Sbrana A. (1999), Shallow and deep reservoirs involved in magma supply of the 1944 eruption of Vesuvius, Bull. Volcanol., 61, 48-63.
Martelli M., Nuccio P. M., Stuart F. M., Di Liberto V., Ellam R. M. (2008), Constraints on mantle source and interactions from He-Sr isotope variation in Italian Plio-Quaternary volcanism, Geochem. Geophys. Geosyst., 9, Q02001, doi:10.1029/2007GC001730.

Mele D., Sulpizio R., Dellino P., La Volpe L. (2011). *Stratigraphy and eruptive dynamics of a pulsating Plinian eruption of Somma-Vesuvius: the Pomici di Mercato (8900 years B.P.)*. Bull. Volcanol., 73, 257-278.

Orsi G., Di Vito M., Isaia R., (eds), 1998. *Volcanic Hazard and Risk in the Parthenopean Megacity*. Int. Meet. "Cities on Volcanoes", Roma and Napoli, Italy, june 28-july 4. Guidebook to field Excursion, Eds. Orsi G., Di Vito M.A., Isaia R., 221pp.

Piochi M., Ayuso R. A., De Vivo B., Somma R. (2006), Crustal contamination and crystal entrapment during polybaric magma evolution at Mt. Somma-Vesuvius Volcano, Italy: Geochemical and Sr isotope evidence, Lithos, 86, 303-329.

Piochi, M., Bruno P.P., De Astis G. (2005), Relative roles of rifting tectonics and magma uprising processes: inferences from geophysical, structural and geochemical data of the Neapolitan volcanic region (southern Italy), Gcubed, 6(7), 1-25, doi:10.1029/2004GC000885.

Quareni, F., Moretti R., Piochi M., Chiodini G. (2007), Modeling of the thermal state of Mount Vesuvius from 1631 A.D. to present and the role of CO_2 degassing on the volcanic conduit closure after the 1944 A.D. eruption, J. Geophys. Res., 112, B03202, doi:10.1029/2005JB003841.

Rolandi, G., Barrella A.M., Borrelli A. (1993), The 1631 eruption of Vesuvius, J. Volcanol. Geotherm. Res., 58, 183-201.

Rosi M., Santacroce R. (1983), The AD 472 Pollena eruption: volcanological and petrological data for this poorly-known, plinian-type event at Vesuvius. J. Volcanol. Geotherm. Res., 17, 249-271.

Santacroce, R. ed (1987), Somma-Vesuvius. Somma-Vesuvius, Quaderni de La Ricerca Scientifica 114, vol 8, CNR Roma, pp 1-251.

Santacroce R, Cioni R, Marianelli P, Sbrana A, Sulpizio R, Zanchetta G, Donahue DJ, Joron JL (2008) Age and whole rock-glass compositions of proximal pyroclastics from the major explosive eruptions of Somma-Vesuvius: a review as a tool for distal tephrostratigraphy. J Volcanol Geotherm Res 177, 1-18.

Santacroce, R., Sbrana A. (eds) (2003), Geological map of Vesuvius. Firenze: SELCA.

Sigurdsson H., Carey S., Cornell W., Pescatore T. (1985), The eruption of Vesuvius in AD 79: Natl. Geogr. Res., 1, 332-387.

Sulpizio, R., Bonasia, R., Dellino, P., Di Vito, M.A., La Volpe, L., Mele, D., Zanchetta, G., Sadori, L. (2008), Discriminating the-long distance dispersal of fine ash from sustained columns or near ground ash clouds: the example of the Pomici di Avellino eruption (Somma-Vesuvius, Italy). J. Volcanol. Geotherm. Res., 177, 265-278, doi:10.1016/j.jvolgeores.2007.11.012.

Sulpizio R, Cioni R, Di Vito MA, Mele D, Bonasia R, Dellino P., 2010. *The Pomici di Avellino eruption of Somma-Vesuvius (3.9 ka BP) part I: stratigraphy, compositional variability and eruptive dynamics.* Bull. Volcanol., 72, 539-558.

Vilardo, G., Ventura G., Milano G. (1999), Factors controlling the seismicity of the Somma-Vesuvius volcanic complex, Volcanol. Seismol., 20, 219- 238.

Zollo A., Gasparini P., Virieux J., Le Meur H., De Natale G., Biella G., Boschi E., Capuano P., De Franco R., Dell'Aversana P., De Matteis R., Guerra I., Iannaccone G., Mirabile L., Vilardo G. (1996), Seismic evidence for a low-velocity zone in the upper crust beneath Mount Vesuvius, Science, 274, 592-594.